A NON-SINGULAR CUMULATIVE DAMAGE MODEL TO PREDICT FATIGUE CRACK GROWTH UNDER SERVICE LOADING

J.T.P. Castro[1], M.A. Meggiolaro[1], A.C.O. Miranda[2]

[1]Mechanical Engineering Department, [2]Tecgraf, Computer Graphics Group
Pontifical Catholic University of Rio de Janeiro (PUC-Rio), Brazil

ABSTRACT

Three classes of mechanisms can cause load sequence effects on fatigue crack growth, depending if they act ***before***, ***at*** or ***after*** the crack tip. Critical Damage is a mechanism of the latter type, where the fatigue cracking is assumed caused by the sequential failure of volume elements (VE) close to the crack tip, calculated by damage accumulation concepts. The crack is treated as a sharp notch, avoiding the unrealistic singularity at its tip. The crack stress concentration factor and a strain concentration rule are used to calculate the notch root strain, which gives a non-singular model for the strain distribution ahead of the crack tip. The damage caused by each load cycle, including the effects of residual stresses, are calculated at each VE using the corrected hysteresis loops caused by the loading. This proposed approach is first validated by comparing the measured with the predicted **da/dN**×**ΔK** curves of three structural alloys. The predictions are made using only **εN**, toughness and threshold properties, since the model does not need any fitting constant. This idea is then extended to predict fatigue crack growth under variable amplitude loading, assuming that the width of the volume element broken at each cycle is equal to the region ahead of the crack tip that suffers damage beyond its critical value.

KEYWORDS: Fatigue, Critical Damage, Crack Growth Modeling, Non-Singular Crack Tip Model

INTRODUCTION

There are many mechanisms that can retard or accelerate the growth of a fatigue crack after significant load amplitude variations [1-3]. Moreover, these mechanisms generally can act simultaneously, with their relative importance in any problem depending on several factors such as crack and piece sizes, dominant stress state at the crack tip, microstructure of the material, mean load, and environment. These load interaction mechanisms can act ***behind***, ***at*** or ***ahead*** of the crack tip, and among them the most important are

- crack closure (***behind*** the crack tip), which can be caused by plasticity, oxidation or roughness of the crack faces, or even by strain induced phase transformation, e.g.,
- crack tip blunting, kinking or bifurcation (***at*** or close to the crack tip), and
- residual stress and strain fields (***ahead*** of the crack tip).

Most models of load sequence effects in fatigue crack growth (FCG) are still based on plasticity-induced crack closure, despite some important limitations. However, there are several important problems that cannot be explained by the effective stress intensity range $\mathbf{\Delta K_{eff}}$ concept. For example, a strong objection [4] against crack closure is based on convincing experimental evidence such as fatigue crack growth threshold values $\mathbf{\Delta K_{th}}$ that are higher in vacuum than in air. Another important problem that cannot be explained by the Elber mechanism is the crack delays or arrests under high $\mathbf{R = K_{min}/K_{max}}$ ratios, when the minimum value $\mathbf{K_{min}}$ of the applied range $\mathbf{\Delta K = K_{max} - K_{min}}$ always remains *above* $\mathbf{K_{op}}$, the (measured) load that opens the fatigue crack [5-6].

THE NON-SINGULAR DAMAGE MODEL

The damage *ahead* of a fatigue crack tip can be estimated using simple but sound hypotheses and standard fatigue calculations, supposing that fatigue cracks grow by sequentially breaking small volume elements (VE) ahead of their tips, which fracture when the crack tip reaches them because they accumulated all the damage the material can support. In this way, **εN** procedures can be combined with fracture mechanics concepts to predict FCG, using the cyclic properties of the material and the strain distribution ahead of the crack tip. These models can consider the VE width in the FCG direction as being the distance that the crack grows on each cycle, or the FCG rate as being the VE width divided by the number of cycles that the crack would need to cross it. Critical damage models are not new [7-13], but still need improvements. Most models assume a singular stress/strain field ahead of the crack tip (concentrating in this way all the damage next to the tip) and need some adjustable constant to fit the FCG **da/dN** data, compromising their prediction potential. But the supposed singularity at the crack tip is a characteristic of the mathematical models that postulate a zero radius tip, not of the real cracks, which have a blunt tip when loaded (and finite strains at their tip, or else they would be unstable).

To avoid this problem, the actual finite strain range at the crack tip $\Delta\varepsilon_{tip}$ can be estimated using the stress concentration factor K_t for the blunt crack [14] and a strain concentration rule. The strain range field ahead of the crack tip can then be upper-bounded by $\Delta\varepsilon_{tip}$ (e.g. by assuming $\Delta\varepsilon_{tip}$ constant where the singular solution would predict strains greater than $\Delta\varepsilon_{tip}$). Supposing that all fatigue damage occurs inside this region next to the tip, the number of cycles N^* associated with $\Delta\varepsilon_{tip}$ can be obtained from Coffin-Manson's rule, and the FCG rate can as the length of this region divided by N^*. But such models have two shortcomings. First, neglecting the fatigue damage elsewhere concentrates it in the very last N^* cycles, a non-conservative hypothesis. Second, assuming an intermittent and not a cycle-by-cycle FCG, although valid in some cases of crazing in polymers, is certainly not true for most metallic structures, as verified by microscopic observations of fatigue striations.

To avoid these limitations, the model proposed here [6, 11-13] uses Schwalbe's modification [8] of the HRR field to represent the strain range distribution ahead of the crack tip, and (ii) removes the crack tip singularity by shifting the origin of the strain field from the crack tip to a point inside the crack, located by matching the tip strain with $\Delta\varepsilon_{tip}$ predicted by a strain concentration rule, such as Neuber [15], Molsky and Glinka [16], or the linear rule [17]. This approach recognizes that the strain range $\Delta\varepsilon(r, \Delta K)$ in an unbroken VE increases and causes damage in each load cycle as the crack tip approaches it, see Figure 1. Therefore, the VE closest to the tip breaks due to the sum of all damages it suffered during the previous load cycles. In this way, the fatigue crack growth rate under constant **ΔK** is modeled by the sequential failure of identical VE ahead of the crack tip.

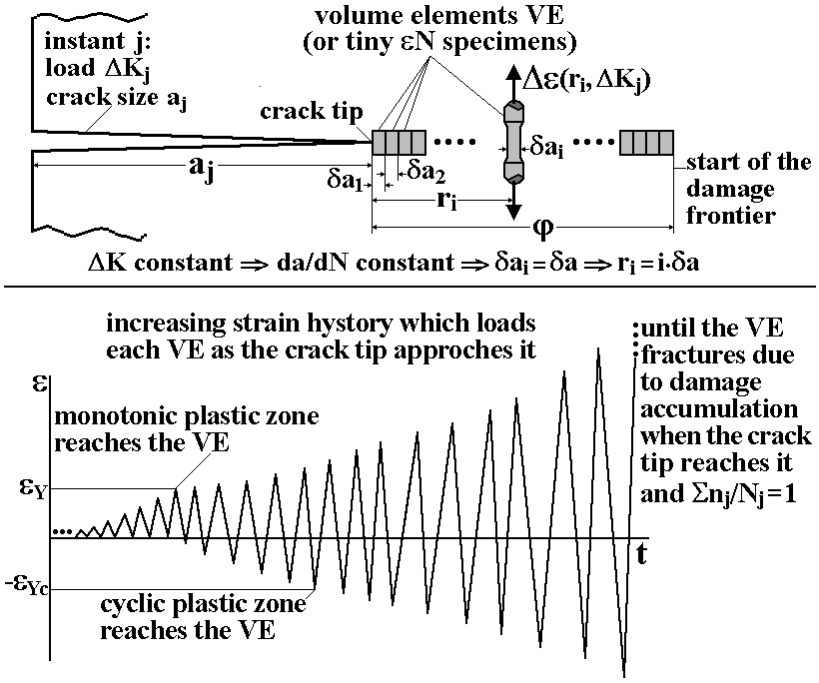

Figure 1: Schematics of the FCG assumed to be caused by the sequential fracture of volume elements (or tiny **εN** specimens) at every load cycle, loaded by an increasing strain history as the crack tip approaches them.

This model is then extended to deal with the VA loading case, which has idiosyncrasies that must be treated appropriately. First, the VE that breaks in any given cycle has variable width, which should be calculated by locating the point ahead of the crack tip where the accumulated damage reaches a specified value (e.g. 1.0 when using Miner's rule). Load sequence effects, such as overload-induced crack growth retardation, are associated with hysteresis loop shifts and with mean load effects on the material **εN** curve, and can be calculated using the powerful numerical tools available in the **ViDa** software [18]. Moreover, this model can recognize an opening load, and thus can separate the cyclic damage from the closure contributions to the crack growth process.

Constant Amplitude Loading

In every load cycle, each VE ahead of the crack tip suffers strain hysteresis loops of increasing range as the tip approaches it, and suffers a damage increment that depends on the strain range in that cycle, thus on $\mathbf{r_i}$, the distance from the i-th VE to the tip and on the load $\mathbf{\Delta K_j}$ at that event. The fracture of a VE near the crack tip occurs when its accumulated damage reaches a critical value, e.g. by Miner's rule, $\mathbf{\Sigma n_j/N_j = 1}$, where $\mathbf{n_j}$ is the number of cycles of the **j**-th load event and $\mathbf{N_j}$ is the number of cycles that the piece would last if loaded solely by that event. If under constant **ΔK** (or $\mathbf{\Delta K_{eff}}$) the fatigue crack advances a fixed distance **δa** in every load cycle, and if, for simplicity, the damage outside the cyclic plastic zone $\mathbf{zp_c}$ is neglected, there are thus $\mathbf{zp_c/\delta a}$ VE ahead of the crack tip at any instant. Since the plastic zone advances with the crack, each new load cycle breaks the VE adjacent to the crack tip, induces an increased strain range in all other unbroken VE, and adds a new element to the damage zone. Thus, as each load cycle causes a growth increment, $\mathbf{n_j = 1}$. Moreover, since the VE are considered as small **εN** specimens, they break when:

$$\sum_{i=0}^{zp_c/\delta a} \frac{1}{N(zp_c - i\cdot\delta a)} = \sum_{r_i=0}^{zp_c} \frac{1}{N(r_i)} = 1 \tag{1}$$

where $\mathbf{N(r_i) = N(zp_c - i\cdot\delta a)}$, the fatigue life corresponding to the plastic strain range $\mathbf{\Delta\varepsilon_p(r_i)}$ acting at a distance $\mathbf{r_i}$ from the crack tip, can be calculated using the plastic part of Coffin-Manson's rule:

$$N(r_i) = \frac{1}{2}\left(\frac{\Delta\varepsilon_p(r_i)}{2\varepsilon_c}\right)^{1/c} \tag{2}$$

$\mathbf{\Delta\varepsilon_p(r_i)}$ in its turn can be described by Schwalbe's [8] modification of the HRR field:

$$\Delta\varepsilon_p(r_i) = \frac{2S_{Yc}}{E}\cdot\left(\frac{zp_c}{r_i}\right)^{\frac{1}{1+h_c}} \tag{3}$$

where $\mathbf{S_{Yc}}$ is the cyclic yield strength, $\mathbf{h_c}$ the Ramberg-Osgood cyclic hardening exponent, and $\mathbf{zp_c}$ is the cyclic plastic zone size in plane strain, which can be estimated, e.g., by [12] (**ν** is Poisson's coefficient):

$$zp_c = \frac{(1-2\nu)^2}{4\pi\cdot(1+h_c)}\cdot\left(\frac{\Delta K}{S_{Yc}}\right)^2 \Rightarrow N(r_i) = \frac{1}{2}\left[\frac{S_{Yc}}{E\varepsilon_c}\cdot\left(\frac{zp_c}{r_i}\right)^{\frac{1}{1+h_c}}\right]^{1/c} \tag{4}$$

The HRR field describes the plastic strains ahead of an idealized crack tip, thus it is singular at $\mathbf{r = 0}$. But an infinite strain is physically impossible (which does not mean that singular models are useless, but only that the damage close to the crack tip is not predictable by them). To eliminate this unrealistic strain singularity, the origin of the HRR coordinate system is shifted into the crack by a small distance **X**, copying Creager and Paris idea [14]. Approximating the VE width **δa** by a differential **da** at a distance **dr** ahead of the crack tip and the Miner's summation by an integral, which is easier to deal with:

$$\Delta\varepsilon_p(r+X) = \frac{2S_{Yc}}{E}\cdot\left(\frac{zp_c}{r+X}\right)^{\frac{1}{1+h_c}} \tag{5}$$

$$\frac{da}{dN} = \int_0^{zp_c} \frac{dr}{N(r+X)} \tag{6}$$

To determine **X** and **N(r + X)** two paths can be followed. The first uses Creager and Paris' **X = ρ/2**, **ρ** being the actual crack tip radius, estimated by **ρ = CTOD/2**, thus

$$\mathbf{X=\frac{\rho}{2}=\frac{CTOD}{4}=\frac{K_{max}^2\cdot(1-2\nu)}{\pi\cdot E\cdot S_{Yc}}\cdot\sqrt{\frac{1}{2(1+h_c)}}} \tag{7}$$

The second path is more reasonable. Instead of arbitrating the strain field origin offset, it determines **X** by first calculating the crack (linear elastic) stress concentration factor $\mathbf{K_t}$ [19]:

$$\mathbf{K_t=2\Delta K/(\Delta\sigma_n\cdot\sqrt{\pi\rho})} \tag{8}$$

For any given **ΔK** and **R** it is possible to calculate **ρ** and $\mathbf{K_t}$ from (7) and (8), and then the strain range $\mathbf{\Delta\varepsilon_{tip}}$ at the crack tip using a strain concentration rule. Assuming that the material stress-strain behavior is parabolic with cyclic strain hardening coefficient $\mathbf{H_c}$ and exponent $\mathbf{h_c}$, with a negligible elastic range, the Linear, Neuber and Molsky and Glinka concentration rules give, respectively:

$$\mathbf{\Delta\varepsilon_{tip}=\frac{K_t\cdot\Delta\sigma_n}{E}=\frac{2\Delta K}{E\sqrt{\pi\cdot CTOD/2}}} \tag{9}$$

$$\begin{cases}\mathbf{\Delta\sigma_{tip}\cdot\Delta\varepsilon_{tip}=\cdot\frac{(K_t\Delta\sigma_n)^2}{E}=\frac{8\Delta K^2}{E\cdot\pi\cdot CTOD}}\\ \mathbf{\Delta\varepsilon_{tip}=2\left(\frac{\Delta\sigma_{tip}}{2H_c}\right)^{1/h_c}}\end{cases} \tag{10}$$

$$\begin{cases}\mathbf{\frac{2\Delta K^2}{E\cdot\pi\cdot CTOD}=\frac{\Delta\sigma_{tip}^2}{4E}+\frac{\Delta\sigma_{tip}}{1+h_c}\cdot\left(\frac{\Delta\sigma_{tip}}{2H_c}\right)^{1/h_c}}\\ \mathbf{\Delta\varepsilon_{tip}=2\left(\frac{\Delta\sigma_{tip}}{2H_c}\right)^{1/h_c}}\end{cases} \tag{11}$$

After calculating $\mathbf{\Delta\varepsilon_{tip}}$ at the crack tip using one of these rules, the shift **X** of the HRR origin is obtained by:

$$\mathbf{\Delta\varepsilon_{tip}=\frac{2S_{Yc}}{E}\cdot\left(\frac{zp_c}{X}\right)^{\frac{1}{1+h_c}}\Rightarrow X=zp_c\cdot\left(\frac{2S_{Yc}}{E\Delta\varepsilon_{tip}}\right)^{1+h_c}} \tag{12}$$

The strain distribution at a distance **r** ahead of the crack tip, $\mathbf{\Delta\varepsilon_p(r + X)}$, without the singularity problem at the crack tip, can now be readily obtained by:

$$\mathbf{\frac{da}{dN}=\int_0^{zp_c}2\cdot\left(\frac{2\varepsilon_c}{\Delta\varepsilon_p(r+X)}\right)^{1/c}dr} \tag{13}$$

This prediction was experimentally verified in SAE1020 and API 5L X-60 steels and in a 7075 T6 Al alloy, using (13) to obtain the constant of a McEvily-type **da/dN** equation, which describes the **da/dN×ΔK** curves using only one adjustable parameter:

$$\mathbf{\frac{da}{dN}=A[\Delta K-\Delta K_{th}(R)]^2\left(\frac{K_c}{K_c-[\Delta K/(1-R)]}\right)} \tag{14}$$

where $\mathbf{K_c}$ and $\mathbf{\Delta K_{th}(R)}$ are the material fracture toughness and crack propagation threshold at the load ratio **R**. To guarantee the consistence of this experimental verification, $\mathbf{K_c}$, $\mathbf{\Delta K_{th}(R)}$, the **εN** and the **da/dN** data were all obtained by testing proper specimens manufactured from the same stock of the 3 materials, following ASTM standards. The API 5L X-60 **da/dN×ΔK** experimental curves is compared with this simple model predictions in Figure 2 (see [6] for the other curves). Both the shape and the magnitude of the data are quite reasonably reproduced by this model, with the Linear rule generating better predictions probably because the tests were made under predominantly plane-ε conditions. Since no adjustable constant was used in this modeling, it can be concluded that this performance is no coincidence.

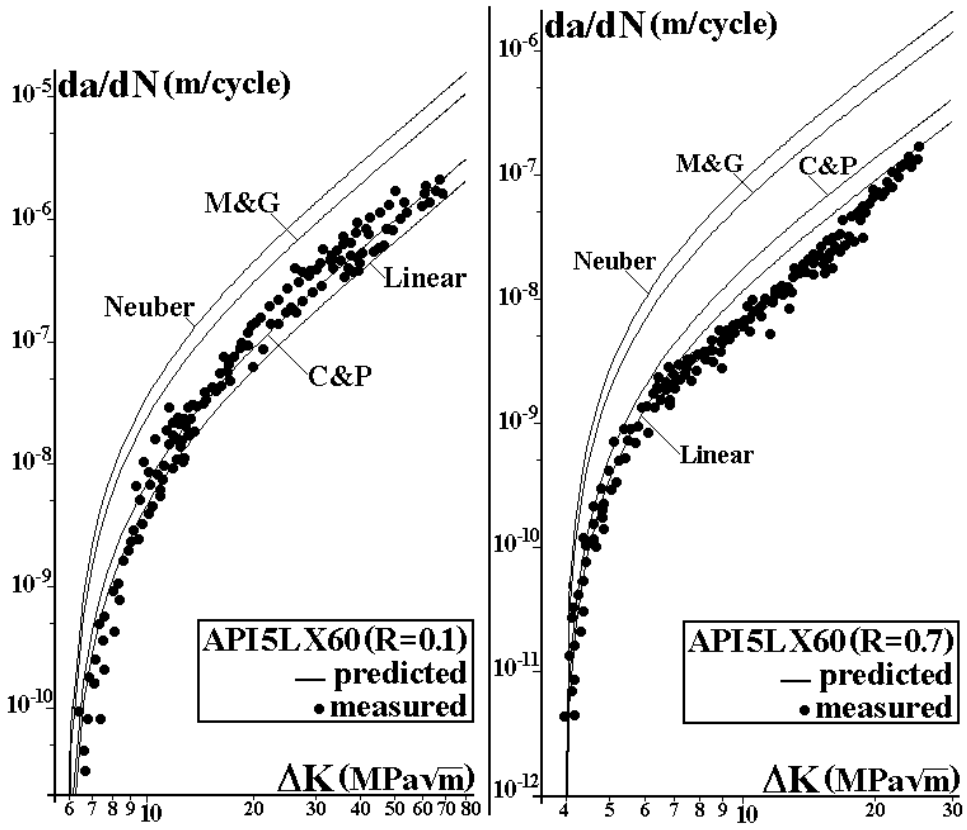

Figure 2: da/dN×ΔK behavior measured and ***predicted*** by the various strain concentration rules used in the critical damage model, for API-5L-X60 pipeline steel at **R = 0.1** and **R = 0.7**.

But some remarks are required. First, damage beyond $\mathbf{zp_c}$ was neglected to simplify the numerical calculations, but as it accumulates at all points ahead of the crack tip, it is wiser to choose the damage origin by numerically testing its influence on **da/dN**, or better by comparing the predictions with FCG tests, as done later on. Second, FE calculations [19] indicate that there is a region adjacent to the blunt crack tip with a strain gradient much lower than predicted by the HRR field. These problems can be avoided by shifting the origin *away* from the tip by $\mathbf{x_2}$ and assuming the crack-tip strain range $\mathbf{\Delta\varepsilon_{tip}}$ constant over the region I of length $\mathbf{x_1+x_2}$ shown in Figure 3. $\mathbf{x_1}$ can be obtained equating $\mathbf{\Delta\varepsilon_{tip}}$ and the HRR-calculated strain range, and the crack-tip stress range $\mathbf{\Delta\sigma_{tip}}$ from:

$$\Delta\sigma_{tip} = \Delta\sigma(r = x_1) = 2S_{Yc} \cdot \left(\frac{zp_c}{x_1}\right)^{\frac{h_c}{1+h_c}} = 2S_{Yc} \cdot \left(\frac{E \cdot \Delta\varepsilon_{tip}}{2S_{Yc}}\right)^{h_c} \tag{15}$$

Then, following Irwin's classical idea, the value of the shift $\mathbf{x_2}$ is obtained by integrating the stress field $\mathbf{\sigma(r)}$, guaranteeing that the shadowed areas below the curves in Figure 40 are the same:

$$\int_0^{\infty} \Delta\sigma(r)dr = \int_0^{x_1+x_2} \Delta\sigma_{tip}dr + \int_{x_1}^{\infty} \Delta\sigma(r)dr \Rightarrow \int_0^{x_1} \Delta\sigma(r)dr = \int_0^{x_1+x_2} \Delta\sigma_{tip}dr \tag{16}$$

Since $\mathbf{x_1 < zp_c}$, $\mathbf{\Delta\sigma(r)}$ in the above integral can be described by the HRR solution, resulting in

$$\int_0^{x_1} 2S_{Yc} \cdot \left(\frac{zp_c}{r}\right)^{\frac{h_c}{1+h_c}} dr = \Delta\sigma_{tip} \cdot x_1 \cdot (1+h_c) = \Delta\sigma_{tip} \cdot (x_1+x_2) \Rightarrow x_2 = x_1 \cdot h_c \tag{17}$$

These simple tricks generate a more reasonable strain distribution model (Figure 3):

$$\Delta\varepsilon(r) = \Delta\varepsilon_{tip}\ ,\ 0 \le r \le x_1 + x_2 \text{ (region I)} \tag{18}$$

$$\Delta\varepsilon(r) = \frac{2S_{Yc}}{E} \cdot \left(\frac{zp_c}{r-x_2}\right)^{\frac{1}{1+h_c}}\ ,\ x_1 + x_2 < r \le zp_c + x_2 \text{ (region II, shifted HRR)} \tag{19}$$

$$\Delta\varepsilon(r) \cong \frac{2S_{Yc}}{E}\cdot\sqrt{\frac{zp_c + x_2}{r}}\cdot\left(1+\nu\frac{r-zp_c}{zp-zp_c}\right),\ zp_c + x_2 < r < zp \text{ (region III, interpolation)} \quad (20)$$

$$\Delta\varepsilon(r) = \frac{\Delta K\cdot(1+\nu)}{\kappa E\sqrt{2\pi(r-zp/2)}},\ r \geq zp \text{ (region IV, shifted Irwin)} \quad (21)$$

where $\kappa = 1$ for plane stress and $\kappa = 1/(1-2\nu)$ for plane strain, and

$$zp = \frac{1}{\pi\kappa^2}\cdot\left(\frac{K_{max}}{S_{Yc}}\right)^2 \text{ and } zp_c = \frac{1}{4\pi\kappa^2\cdot(1+h_c)}\cdot\left(\frac{\Delta K}{S_{Yc}}\right)^2 \quad (22)$$

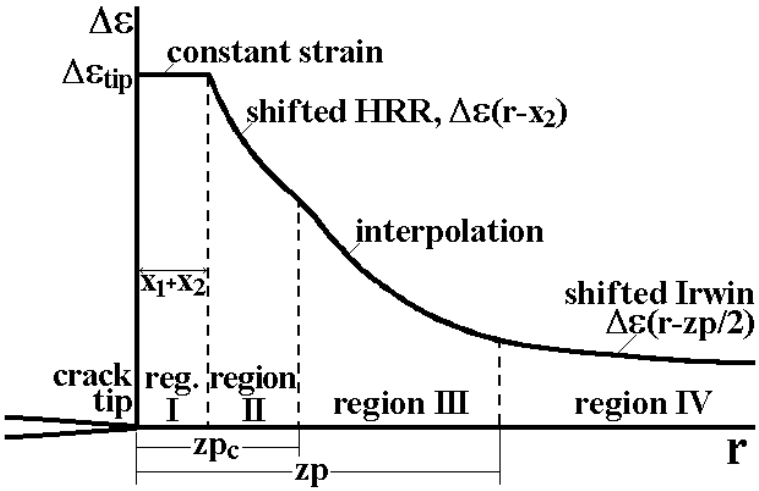

Figure 3: Proposed strain range distribution, divided in 4 regions to consider both the elastic and the plastic contributions to the damage ahead of the crack tip.

Both CA and VA FCG can then be calculated using equations (18-22), which consider all the damage ahead of the crack tip and provide a more realistic model of the FCG process. But (2), (5) and (13) must be modified to include elastic parameters σ_c and **b**, and to account for the mean load σ_m effects on the VE life using Morrow elastic, Morrow elastic-plastic or Smith-Topper-Watson equations. But the life **N** in these equations cannot be explicitly written as a function of the VE strain range and mean load and thus must be calculated numerically, a programming task that, despite introducing no major conceptual difficulty, is far from trivial [18].

Variable Amplitude Loading

The **da/dN×ΔK** curve predicted for CA can be used with some load interaction engineering model in the **ViDa** software for VA problems. But the idea here is to *directly* quantify the fatigue damage induced by the VA load considering the crack growth as caused by the sequential fracture of *variable* size VE ahead of the crack tip. Since the Linear strain concentration rule generated better predictions above, it is the only one used here, and as load interaction effects can have a significant importance in FCG, they are modeled by using Morrow elastic equation to describe the VE fatigue life:

$$N(r+X) = \frac{1}{2}\left(\frac{\Delta\varepsilon_p(r+X)}{2\varepsilon_c}\left(1-\frac{\sigma_m}{\sigma_c}\right)^{-c/b}\right)^{1/c} \quad (23)$$

To account for mean load effects, a modified stress intensity range can be easily implemented for $R > 0$ to filter the loading cycles that cause no damage by using:

$$\Delta K_{eff} = K_{max} - K_{PR} = \frac{\Delta K}{1-R} - K_{PR} \quad (24)$$

where K_{PR} is a propagation threshold that depends on the considered retardation mechanism, such as K_{op} or K_{max}^* from the Unified Approach [4]. The damage function for each cycle is then:

$$d_i(r+X_i) = \frac{n_i}{N_i(r+X_i)} \quad (25)$$

If the material ahead of the crack is supposed virgin, then its increment δa_1 caused by the first load event is the value $r = r_1$ that makes Equation (30) equal to one, therefore:

$$d_1(r_1 + X_1) = 1 \quad \Rightarrow \quad \delta a_1 = r_1 \tag{26}$$

In all subsequent events, the crack increments take into account the damage accumulated by the previous loading, in the same way it was done for the constant loading case. But as the coordinate system moves with the crack, a coordinate transformation of the damage functions is necessary:

$$D_i = \sum_{j=1}^{i} d_j \left(r + \sum_{p=j}^{i-1} \delta a_p \right) \tag{27}$$

Since the distance $r = r_i$ where the accumulated damage equals one in the **i**-th event is a variable that depends on ΔK_i (or ΔK_{eff_i}) and on the previous loading history, VE of different widths may be broken at the crack tip by this model. This idea is illustrated by the events schematized in Figure 4.

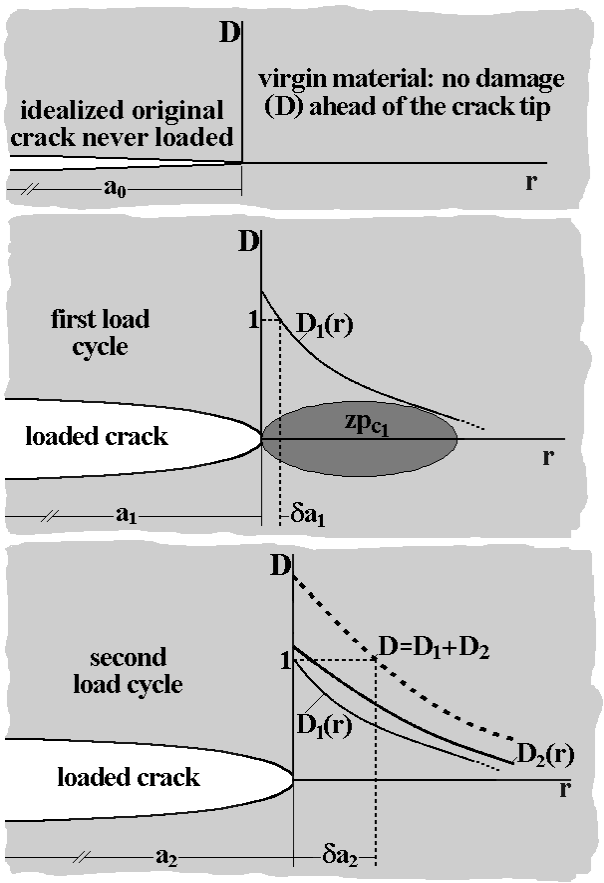

Figure 4: Schematics of the critical damage calculations, which under variable amplitude loading recognize variable crack increments by forcing the crack to grow over the region where **D = 1**.

RESULTS AND DISCUSSIONS

FCG tests under VA loading were performed on API-5L-X52 steel **50×10mm** C(T) specimens, pre-cracked under CA at $\Delta K = 20MPa\sqrt{m}$ until reaching crack sizes $a \cong 12.6mm$. These cracks were measured within **20μm** accuracy by optical methods and by a strain gage bonded at the back face of the C(T). The basic monotonic and cyclic properties, measured in computer-controlled servo-hydraulic machines using standard ASTM testing procedures, are $E = 200 \cdot 10^3$, $S_U = 527$, $S_Y = 430$, $S_{Yc} = 370$, $H_c = 840$, and $\sigma_c = 720$ (all in MPa), $h_c = 0.132$, $\varepsilon_c = 0.31$, $b = -0.076$ and $c = -0.53$. About 50 specimens were tested under deformation ratios varying from $R = -1$ to $R = 0.8$ (at least 2 at each strain range) to obtain the **εN** curve, see Figure 5. Morrow's strain-life equation (25), which includes the mean stress effect only in Coffin-Manson's elastic term, best fit the experimental data. The basic **da/dN** curve, measured using the same equipment, is fitted by $da/dN(R = 0.1) = 2 \cdot 10^{-10}(\Delta K - 8)^{2.4}$ (in **m/cycle**), where $\Delta K_{th}(R = 0.1) = 8MPa\sqrt{m}$.

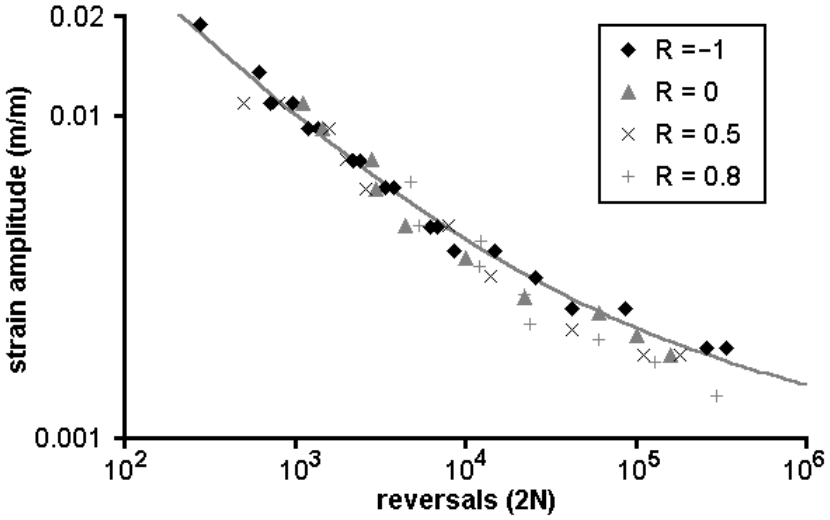

Figure 5: API 5L X52 steel measured strain-life data, and Morrow elastic model that best fitted this data.

FCG tests were then conducted under several VA histories. The history shown in Figure 6 has 50,000 blocks containing 100 reversals each. The high mean stress levels were chosen to avoid crack closure effects. The load history was counted by the sequential rain-flow method, using the **ViDa** software [18]. The damage calculation was made using a specially developed code following all the procedures discussed above. The crack growth predictions based solely on **εN** parameters are again quite reasonable, see Figure 7. The prediction assuming no damage outside the cyclic plastic zone $\mathbf{zp_c}$ underestimated the crack growth. However, when the small (but significant) damage in the material between the cyclic and monotonic plastic zone borders is also included in the calculations, an even better agreement is obtained. Note also that crack growth is slightly underestimated after $1.8{\cdot}10^6$ cycles, probably due to having neglected the elastic damage and the (small) mean stress effects.

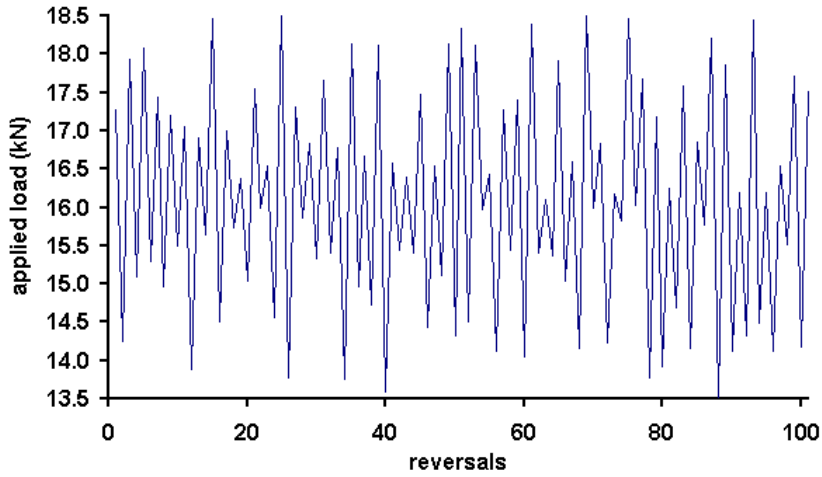

Figure 6: Variable amplitude load block applied to the API-5L-X52 steel C(T). Note the high mean R-ratio.

A similar test was conducted on AISI 1020 steel, with measured properties $\mathbf{E = 205GPa}$, $\mathbf{S_U = 491}$, $\mathbf{S_Y = 285}$, $\mathbf{S_{Yc} = 270}$, $\mathbf{H_c = 941}$ and $\mathbf{\sigma_c = 815MPa}$, $\mathbf{h_c = 0.18}$, $\mathbf{\varepsilon_c = 0.25}$, $\mathbf{b = -0.114}$, and $\mathbf{c = -0.54}$. The FCG curve fit is $\mathbf{da/dN = 5{\cdot}10^{-10}{\cdot}(\Delta K - \Delta K_{th})^2{\cdot}\{K_c/[K_c - \Delta K/(1-R)]\}}$, where $\mathbf{\Delta K_{th} = 11.6}$ and $\mathbf{K_c = 277}$ ($\mathbf{\Delta K}$, $\mathbf{\Delta K_{th}}$ and $\mathbf{K_c}$ in $\mathbf{MPa\sqrt{m}}$ and **da/dN** in **m/cycle**). The VA load history is a series of blocks containing 101 peaks and valleys, as shown in Figure 8, with a duration of two seconds each. Figure 9 compares the predictions with the measured data. This other prediction of fatigue crack growth under VA based only on εN properties turns out to be again quite accurate. Therefore, these tests indicate that the ideas behind the proposed critical damage model make sense and deserve to be better explored.

CONCLUSIONS

Several mechanisms can cause load sequence effects on fatigue crack growth, and they may act *before*, *at* or *after* the crack tip. Plasticity-induced crack closure is the most popular of them, but it cannot explain sequence

effects in various important problems. A damage accumulation model ahead of the crack tip based on εN cyclic properties, which can explain those effects in the absence of closure, was proposed for predicting fatigue crack propagation under variable amplitude loading. The model treats the crack as a sharp notch with a small but finite radius to avoid singularity problems, and calculates damage accumulation explicitly at each load cycle. Experimental results show a good agreement between measured crack growth both under constant and variable amplitude loading and the predictions based purely on εN data.

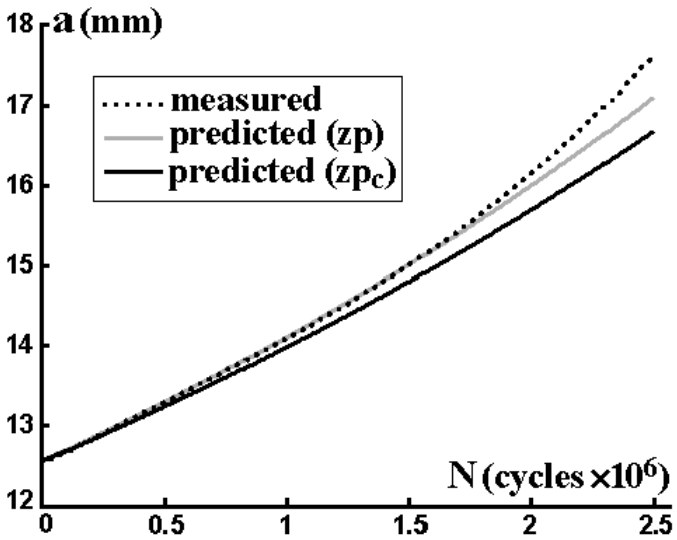

Figure 7: Comparison between the crack growth measurements and the εN-based predictions for the variable amplitude load presented in Figure 44 (API-5L-X52 steel).

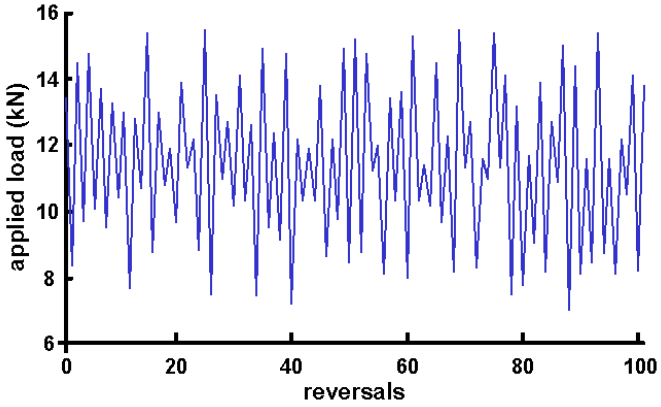

Figure 8: VA load block applied to the SAE 1020 steel C(T). Again a high mean R-ratio was used in this test, to avoid the interference of possible significant closure effects which could mask the model performance.

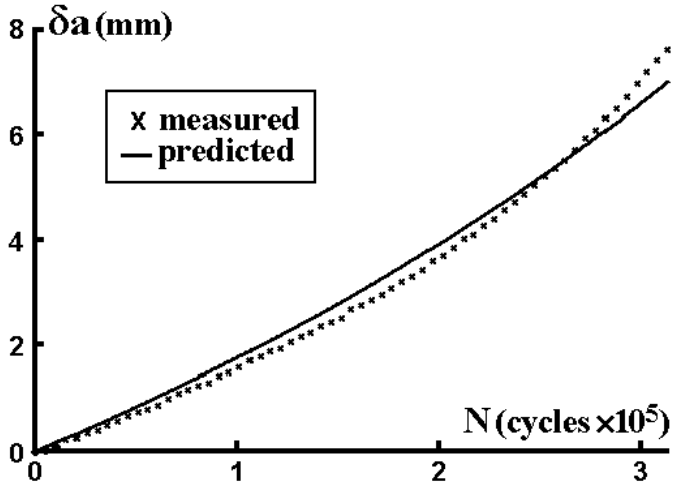

Figure 9: Comparison between the crack growth measurements and the εN-based predictions for the variable amplitude load presented in Figure 46 (SAE 1020 steel).

REFERENCES

1. Suresh, S. (1998), *Fatigue of Materials*, 2nd ed., Cambridge
2. Skorupa, M. (1998), *Fatigue and Fracture of Engineering Materials and Structures* 21, 987
3. Skorupa, M. (1999), *Fatigue and Fracture of Engineering Materials and Structures* 22, 905
4. Sadananda, K., Vasudevan, A.K. and Holtz, R.L. (2001), *International Journal of Fatigue* 23, S277
5. Meggiolaro, M.A. and Castro, J.T.P. (2003), *International Journal of Fatigue* 25, 843
6. Castro, J.T.P., Meggiolaro, M.A. and Miranda, A.C.O. (2005), *International Journal of Fatigue* 27, 1366
7. Majumdar, S. and Morrow, J. (1974), *ASTM STP 559*, 159
8. Schwalbe, K.H. (1974), *Engineering Fracture Mechanics* 6, 325
9. Glinka, G. (1982), *International Journal of Fatigue* 4, 59
10. Glinka, G. (1985),*Engineering Fracture Mechanics* 21, 245
11. Castro, J.T.P. and Kenedi, P.P. (1995), *Journal of the Brazilian Society of Mechanical Sciences* 17, 292
12. Durán, J.A.R., Castro, J.T.P. and Payão Filho, J.C. (2003), *FFEMS* 26, 137
13. Durán, J.A.R., Castro, J.T.P. and Meggiolaro, M.A. (2002), in *Fatigue 2002* pp.2759, , Blom,AF ed., Emas
14. Creager, M. and Paris, P.C. (1967), *International Journal of Fracture Mechanics* 3, 247
15. Neuber, H. (1961), *Journal of Applied Mechanics* 28, 544
16. Molsky, K. and Glinka, G. (1981), *Materials Science and Engineering* 50, 93
17. Stephens, R., Fatemi, A., Stephens, R.R. and Fuchs, H.O. (2000) *Metal Fatigue in Engineering*, Interscience
18. www.tecgraf.puc-rio.br/vida
19. Parton, V.Z. and Morozov, E.M. (1978) *Elastic-Plastic Fracture Mechanics*, Mir Publishers, Moscow